Direct Reduction of Siderite Ore Combined with Catalytic CO/CO_2 Hydrogenation to Methane and Methanol: A Technology Concept

Sascha Kleiber[1], Astrid Loder[1], Matthäus Siebenhofer[1], Andreas Böhm[2], and Susanne Lux[1,*]

DOI: 10.1002/cite.202100189

Supporting Information available online

Industrial CO_2 emission mitigation necessitates holistic technology concepts; especially in high-emission industrial sectors like the iron and steel industry. A novel direct reduction technology with hydrogen reduces CO_2 emissions in iron production from siderite ore by more than 60 %. Subsequent valorization of the process gas, consisting of unconverted hydrogen, carbon monoxide, and CO_2, by catalytic hydrogenation to methane and methanol completes the technology concept. This route gives access to CO_2 emission-lean iron production from siderite ore, fossil-free methane and methanol synthesis, and thus, improved energy density of the energy carrier hydrogen.

Keywords: Direct reduction, Hydrogen, Methanation, Methanol, Siderite

Received: October 20, 2021; *revised:* February 18, 2022; *accepted:* March 07, 2022

1 Introduction

Carbon dioxide (CO_2) emission mitigation is a topic of global concern. Industry accounts for one third of overall anthropogenic CO_2 emissions, and in turn, iron and steel production is responsible for 13–25 % of the industrial sector's contribution [1]. Even though the global industrial CO_2 emissions reduced by 37 % from 1376.4 $Mt_{CO_2\,eq}a^{-1}$ in 1990 to 866.1 $Mt_{CO_2\,eq}a^{-1}$ in 2014, the CO_2 concentration in the atmosphere has continued to increase. In 2019, the average CO_2 concentration in the atmosphere was 410 ppm [1, 2]. Global steel production increased from 1.44 Gt in 2010 to 1.88 Gt in 2020 [2]. The total Austrian production was 5.3 Mt of pig iron and 6.8 Mt of crude steel in 2020 [3].

The Austrian iron and steel production rely beside imported iron oxide ore on mineral iron carbonate from the deposit at the Erzberg in Styria (Austria). This mineral iron carbonate, hereinafter referred to as siderite ore, consists of three main carbonate components. These are the two iron-bearing components siderite, $FeCO_3$ with partial Mg and Mn substitution, and ankerite $(Ca_aFe_bMg_cMn_d)CO_3$ as well as dolomite $(Ca,Mg)(CO_3)_2$. Due to its carbonate character, processing of siderite ore is challenging. The state-of-the-art process is based on a two-step route with calcination in a sinter plant and consecutive reduction in the blast furnace. In the first step, siderite is calcinated in air to release CO_2 and form hematite (Fe_2O_3, Eq. (1)). In the second step, hematite is reduced to pig iron in the blast furnace using carbon monoxide (CO) from coke as reducing agent (Eq. (2)).

$$4FeCO_3 + O_2 \rightarrow 2Fe_2O_3 + 4CO_2 \quad \Delta_R H^0 = -261\ \text{kJ mol}^{-1} \tag{1}$$

$$Fe_2O_3 + 3CO \rightarrow 2Fe + 3CO_2 \quad \Delta_R H^0 = -24\ \text{kJ mol}^{-1} \tag{2}$$

This process emits 1.8–2.0 t CO_2 per t steel by the use of coke to provide the reducing agent and as energy source [4]. It is not expected that steel production and demand will decrease significantly on a global scale within the 21st century. Thus, the search for measures to substantially reduce the high level of CO_2 emissions in the iron and steel industry is a high priority task. Basically, it is conceivable to

[1]Sascha Kleiber, Astrid Loder, Prof. Dr. Matthäus Siebenhofer, Prof. Dr. Susanne Lux
susanne.lux@tugraz.at
Graz University of Technology, NAWI Graz, Institute of Chemical Engineering and Environmental Technology, Inffeldgasse 25/C, 8010 Graz, Austria.

[2]Prof. Dr. Andreas Böhm
Montanuniversität Leoben, Institute of Mineral Processing, Franz Josef-Straße 18, 8700 Leoben, Austria.

increase steel recycling and scrap use. Though an increase of steel recycling is expected, it will not be sufficient to cover the demand – projections estimate that recycled steel will meet 44 % of the total steel demand by 2050 [5]. A combined approach of maximizing steel recycling from scrap and new low-emission iron and steelmaking technologies from iron ore, so-called CO_2 breakthrough technologies, is urgently needed to meet the demand of substantially less CO_2 emissions.

A promising alternative to the conventional two-step process is the direct reduction of siderite ore with hydrogen (H_2) in one process step (Eq. (3), simplified reaction equation without consideration of reduced carbon species) [6–8]. The use of hydrogen is highly promoted for sustainable, future-oriented iron and steel production. However, until now mainly the reduction of iron oxide ore has been considered. For siderite ore, this implies oxidation to hematite and, thus, transfer from oxidation state Fe^{+2} to oxidation state Fe^{+3}, prior to reduction to elemental iron $Fe^{\pm0}$. When iron carbonate (Fe^{+2}) is directly reduced to elemental iron, this reduces the amount of the necessary reducing agent hydrogen by 33 % and lowers CO_2 emissions by more than 60 %; simply due to the reaction stoichiometry. The process gas of the direct reduction of siderite ore does not only consist of the released CO_2 but is partially upgraded by in-situ formation of reduced carbon species, such as CO, methane (CH_4), and methanol (CH_3OH) (Eq. (4)), together with excess hydrogen [7, 9]. The individual reaction equations for dedicated product formation and their standard reaction enthalpies $\Delta_R H^0$ at 298 K can be found in the Supporting Information.

$$FeCO_3 + H_2 \rightarrow Fe + H_2O + CO_2 \quad \Delta_R H^0 = 61\ \text{kJ mol}^{-1} \tag{3}$$

$$(a+b)FeCO_3 + \left[(a+b)\left(\frac{c}{2}+d\right)+b\right]H_2 \rightarrow aFeO + bFe + (a+b)CH_cO_{2-d} + [b+d(a+b)]H_2O \tag{4}$$

To further reduce CO_2 emissions and establish a CO_2 emission-lean pathway for iron production from siderite ore, a holistic technology concept is required. Besides the origin of the reducing agent hydrogen, further use of the process gas from the direct reduction step needs to be considered. Possible sources for green hydrogen are the electrolysis of water with excess energy from wind and solar power plants at peak production times, and photocatalytic water splitting with sunlight and ruthenium catalysts [10]. Suitable valorization strategies to upgrade the CO/CO_2-rich process gas are catalytic CO/CO_2 hydrogenation to methane and methanol. Methane and methanol synthesis through CO/CO_2 hydrogenation can handle a wide range of feed gas compositions and are capable of achieving high carbon-based conversions and product selectivities. Methane and methanol easily release hydrogen by steam reforming, making them highly feasible for fuel cell powering. Existing distribution networks such as natural gas pipelines and fuel stations could be used to provide methane and methanol for customers. Further, they can be used as marine fuel [11, 12] and to provide electricity in remote regions, as gas turbines successfully run on methane and methanol [13, 14]. Besides its usage as a solvent for paints, plastics, and adhesives, the bulk chemical methanol is feedstock for the production of many chemicals, such as formaldehyde, ethylene, propylene, methyl tertiary-butyl ether, and acetic acid.

The efficiency of catalytic CO and CO_2 hydrogenation highly depends on the choice of the catalyst. Ni-based catalysts have proven successful for methane synthesis [15, 16], whereas Cu-based catalysts have been applied for methanol synthesis [17–20]. To close the raw material cycle and provide a complete technology concept for iron production based on the direct reduction of siderite ore, MgO stands out as a suitable carrier material for the catalytically active components Ni and Cu. Due to its CO_2 adsorption capacity it gives access to bifunctional catalysts [21–25]. At the end of their lifetime, the spent Ni/MgO and Cu/MgO catalysts from methane and methanol synthesis, respectively, can easily be recycled in the blast-oxygen furnaces in the steel and copper industry, as MgO acts as a suitable slag-former.

So far, all process steps have been examined and reported individually. The aim of this paper is to put the findings to date into a broader context, to combine them and illustrate a holistic technology concept. The concept is based on direct reduction of siderite ore with hydrogen, followed by valorization of the process gas through CO/CO_2 hydrogenation to methane or methanol. The proposed concept provides a CO_2 emission-lean alternative to the conventional two-step pig iron production process of siderite ore calcination in the sinter plant followed by reduction in the blast furnace (Fig. 1).

2 Direct Reduction of Siderite Ore with Hydrogen

Mineral iron carbonate from the Austrian Erzberg consists of two iron-bearing components, siderite and ankerite. Both iron-bearing species can be reduced to elemental iron in hydrogen atmosphere at relatively low temperatures of 673–773 K [6–8]. The concomitant carbonates, magnesium carbonate, manganese carbonate, and calcium carbonate, are calcined to their respective oxides. Direct reduction with hydrogen yields a high degree of metallization ($w_{Fe,met}$), meaning the content of elemental iron ($m_{Fe,met}$) based on the total iron content in the ore ($m_{Fe,tot}$, Eq. (5)) [26].

$$w_{Fe,met} = \frac{m_{Fe,met}}{m_{Fe,tot}} \tag{5}$$

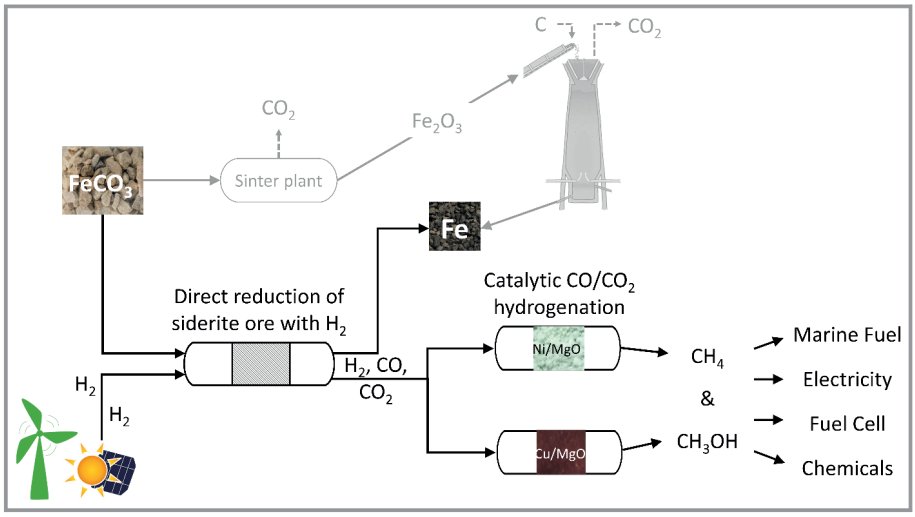

Figure 1. Technology concept for CO_2 emission-lean iron production through direct reduction of siderite ore with hydrogen and valorization of the process gas through catalytic CO/CO_2 hydrogenation to methane and methanol; for comparison: conventional two-step pig iron production process through calcination of siderite ore to hematite in a sinter plant and consecutive reduction in the blast furnace.

2.1 Materials and Methods – Direct Siderite Reduction

The total iron content of the siderite ore sample from the Austrian Erzberg was 33.56 wt %. A size fraction of 0.5–1 mm out of manual screen analysis was used for the experiments. The experiments were performed in a stainless steel fixed-bed tubular reactor (Parr Instrument Company) with a reactor length of 800 mm and an inner diameter of 25 mm in semi-continuous mode. 100 g of the siderite ore sample were placed in the middle of the reactor. The feed gas composition (H_2/N_2 = 90:10 (v/v)) at the reactor inlet was adjusted by two mass flow controllers. A feed gas flow rate of 0.048 m^3h^{-1} (STP) was used. The reactor was equipped with a heating jacket. The temperature inside the reactor was measured by six thermocouples. The process gas stream was cooled at the reactor exit with two heat exchangers (set to 273 K). Water was the only condensable product, which was separated from the gas stream in two condensate tanks. The dry product gas was analyzed by a multi gas analyzer (ABB Uras26 for CO_2, CO, and CH_4; ABB Caldos27 for H_2). A detailed description of the experimental setup and procedure is given in Loder et al. [26].

2.2 Results – Direct Siderite Reduction

For industrial implementation, temperatures of 873–1023 K are sufficient for direct reduction of siderite ore with hydrogen. The experimental studies in the lab-scale fixed-bed tubular reactor have shown that complete $FeCO_3$ conversion from siderite and ankerite is possible with a degree of metallization of > 80 % at a temperature of 873 K (reduction time of 5.6 h). The remaining iron was present as partially reduced wüstite ($Fe_{1-x}O$) [26]. Increasing the reduction temperature above 873 K resulted in an increase of the degree of metallization up to 92 % at 1023 K, while the reduction time decreased to 2.5 h. The reduction was stopped when the process gas composition at the reactor exit ($\varphi_{Process\ gas}$) was indistinguishable from the feed gas composition (φ_{Feed}). The effect of the reduction temperature on the reduction time until no further change in composition in the process gas stream was noticeable is depicted in Fig. 2. Below 873 K, $FeCO_3$ from siderite and ankerite was only partly converted. Exceeding the reduction time at 873 K from 5.6 h up to 11 h did not show any significant effect on the degree of metallization (Fig. 3).

High flexibility concerning the availability of the reducing agent hydrogen is crucial to establish a technology concept for the production of iron through direct reduction of siderite ore with hydrogen. The flexibility of the direct reduction process regarding the hydrogen concentration in the feed gas stream was investigated by Loder et al. [26] through variation of the feed gas ratio of hydrogen to nitrogen (H_2/N_2) from 90:10 to 55:45 (v/v), and the admixture of

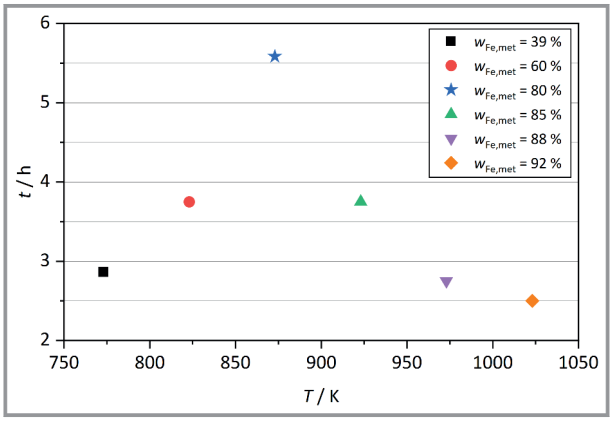

Figure 2. Effect of the reduction temperature on the reduction time until the process gas composition at the reactor exit is indistinguishable from the feed gas composition. Process conditions: fixed-bed tubular reactor, feed gas ratio of H_2/N_2 = 90:10 (v/v), feed gas flow rate $\dot{V}_{Feed}$ = 0.048 $m^3\,h^{-1}$ (STP), mass of siderite ore m_{Sid} = 100 g, ambient pressure. The temperature is shown as mean values with a standard deviation of ±0.8 %.

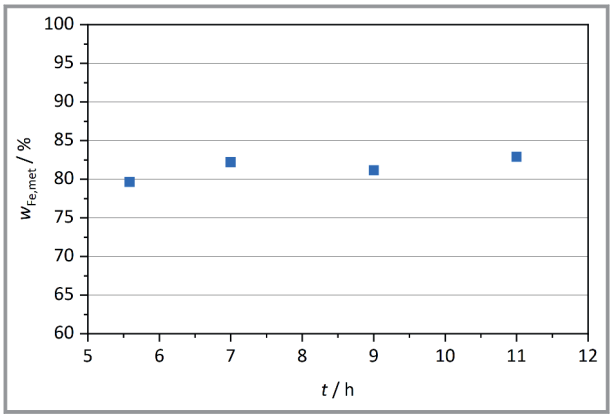

Figure 3. Effect of increased reduction time on the degree of metallization for direct reduction of siderite ore with hydrogen at 873 K. Process conditions: fixed-bed tubular reactor, feed gas ratio of H_2/N_2 = 90:10 (v/v), feed gas flow rate $\dot{V}_{Feed}$ = 0.048 m^3h^{-1} (STP), mass of siderite ore m_{Sid} = 100 g, ambient pressure.

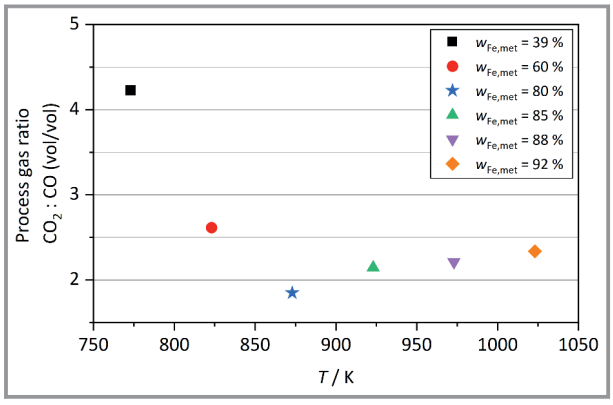

Figure 4. Effect of the reduction temperature on the process gas ratio of CO_2/CO for direct reduction of siderite ore with hydrogen. Process conditions: fixed-bed tubular reactor, feed gas ratio of H_2/N_2 = 90:10 (v/v), feed gas flow rate $\dot{V}_{Feed}$ = 0.048 m^3h^{-1} (STP), mass of siderite ore m_{Sid} = 100 g, ambient pressure. The temperature is shown as mean values with a standard deviation of ±0.8 %. The process gas ratio of CO_2/CO is also shown as mean values with a standard deviation of ±1.5 %.

methane (15–80 vol %) and CO_2 (27–63 vol %) to the feed gas stream. The degree of metallization did not vary significantly with varying hydrogen concentration and methane admixture, implying a high flexibility of the process for fluctuating hydrogen availability. Admixture of CO_2 to the feed gas favored magnetite (Fe_3O_4) formation and, thereby, decreased the degree of metallization significantly.

The composition of the process gas from the direct reduction process is important for its further utilization. A tailor-made process gas composition is possible through precise adaption of the process parameters reduction temperature, pressure, and feed gas composition. Higher reduction temperature and low pressure favor CO formation, whereas methane formation is favored at lower temperature and high pressure [7]. At atmospheric pressure, methane and methanol formation are negligible (below 0.05 vol %). The temperature influence on the total ratio of CO_2/CO released in the process gas at ambient pressure is depicted in Fig. 4. At 873 K, which was the lowest temperature for complete $FeCO_3$ conversion under the conditions investigated, the lowest CO_2/CO ratio of 1.8:1 was observed. With increasing reduction temperature, the process gas ratio of CO_2/CO increased to a value of 2.3:1 at 1023 K. Below 873 K, $FeCO_3$ from siderite and ankerite was only partly converted, and the CO_2/CO ratio was significantly higher with 4.2:1 and 2.6:1 at 773 K and 823 K, respectively.

Based on the experimental studies in the lab-scale fixed-bed tubular reactor in semi-continuous mode (fixed siderite ore sample, continuous feed gas supply), the process gas composition along a continuous reduction reactor was simulated. In the experimental study, siderite ore was reduced with a degree of metallization of 92 % in a feed gas stream with a ratio of H_2/N_2 of 90:10 (v/v) for 2.5 h at 1023 K. Plug flow behavior with continuous co-current supply of siderite ore and feed gas was assumed. Fig. 5 depicts the process gas composition over the residence time in the reactor (= reduction time). Under these process conditions, siderite ore conversion to elemental iron and wüstite is complete and a degree of metallization of 92 % is obtained. The process gas contains 76.0 vol % H_2, 10.1 vol % N_2, 9.7 vol % CO_2, 4.1 vol % CO, and traces of methane (below 0.05 vol %). At steady-state operation, the simulated process

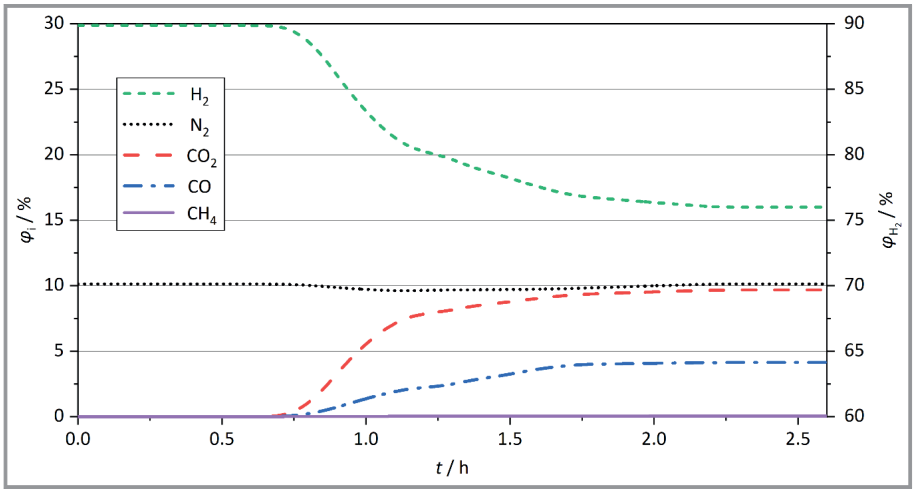

Figure 5. Simulated process gas composition along a continuous reduction reactor. Process conditions: co-current supply of siderite ore and feed gas with a ratio of H_2/N_2 = 90:10 (v/v), degree of metallization $w_{Fe,met}$ = 92 %, ambient pressure.

gas from the continuous reduction reactor adopts a ratio of CO_2/CO of 2.3:1.

To fulfill the requirement of CO_2 emission-lean iron production, the process gas composition may be adapted by varying the process parameters temperature, pressure, and feed gas composition in a first step. In a second step, the process gas may further be upgraded through methane synthesis or methanol synthesis by catalytic CO and CO_2 hydrogenation.

3 Process Gas Valorization

Changing the iron production route with siderite ore from the conventional two-step process to the direct reduction technology reduces the CO_2 emissions by more than 60 %, solely due to the stoichiometry of reaction. However, to further mitigate CO_2 emissions, it is necessary to utilize and upgrade the process gas, which contains unconverted hydrogen, CO_2, CO, and traces of methane, besides, if present, the inert component nitrogen. The high concentration of unconverted hydrogen in the process gas is predestined for its use for catalytic CO and CO_2 hydrogenation. Methane and methanol are potential hydrogenation products. Methane synthesis from CO and CO_2 is extensively discussed in the literature, as it provides a possible route for renewable energy storage [15, 16, 21, 22, 27]. Methanol is a bulk chemical with an annual production rate of 90 million tons [28]. Apart from its role as energy carrier, it is used as a solvent and feedstock for the production of chemicals. State-of-the-art methanol production relies mainly on syngas conversion, which origins from fossil fuels. A shift towards CO_2 as raw material is inevitable for sustainable methanol synthesis.

The hydrogenation reactions of CO and CO_2 to methane (Eqs. (6) and (7)) and methanol (Eqs. (8) and (9)) are both exothermic and volumetric contractive. A partial reduction of CO_2 to CO via the endothermic reverse water-gas shift (RWGS) reaction is, especially for methanol synthesis, an unwanted side reaction (Eq. (10)).

$$CO + 3H_2 \rightleftharpoons CH_4 + H_2O \quad \Delta_R H^0 = -206\ \text{kJ mol}^{-1} \tag{6}$$

$$CO_2 + 4H_2 \rightleftharpoons CH_4 + 2H_2O \quad \Delta_R H^0 = -165\ \text{kJ mol}^{-1} \tag{7}$$

$$CO + 2H_2 \rightleftharpoons CH_3OH \quad \Delta_R H^0 = -91\ \text{kJ mol}^{-1} \tag{8}$$

$$CO_2 + 3H_2 \rightleftharpoons CH_3OH + H_2O \quad \Delta_R H^0 = -50\ \text{kJ mol}^{-1} \tag{9}$$

$$CO_2 + H_2 \rightleftharpoons CO + H_2O \quad \Delta_R H^0 = 41\ \text{kJ mol}^{-1} \tag{10}$$

For industrial application, high CO/CO_2 conversions and high product selectivity are required. Besides the appropriate choice of catalyst, the process conditions need to be chosen according to the chemical thermodynamics of the preferred reaction pathway. In Fig. 6, the standard Gibbs free energies of reaction ($\Delta_R G_T^0$) are depicted for the hydrogenation of CO and CO_2 to methane and methanol and the RWGS reaction in a temperature range of 273 K to 1273 K. The basic challenge for methanol synthesis by CO and CO_2 hydrogenation are the positive $\Delta_R G_T^0$ values above 409 K for CO hydrogenation and throughout the whole temperature range for CO_2 hydrogenation. For methane synthesis from CO and CO_2, $\Delta_R G_T^0$ is negative up to 893 K and 864 K, respectively. According to the principle of Le Chatelier, high pressure and low temperature favor CO and CO_2 hydrogenation to methane and methanol. Especially for methanol synthesis, the choice of specific reaction conditions to increase the reactant conversion and product selectivity is highly important for its economic success.

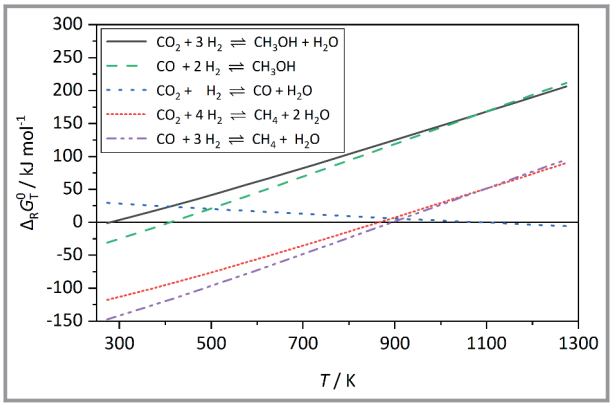

Figure 6. Standard Gibbs free energies of reaction ($\Delta_R G_T^0$) for the reverse water-gas shift (RWGS) reaction and the hydrogenation of CO and CO_2 to methane and methanol; data calculated with HSC Chemistry 8 [29].

The feed gas composition is a further crucial factor. Even though the composition of the process gas from the direct reduction step can be tailored in a wide range, it is governed by the optimum operating conditions for a high degree of metallization and complete $FeCO_3$ conversion. Thus, it differs from the industrial feed gas composition for conventional methanol synthesis, where syngas with a high CO and low CO_2 content is converted over Cu/ZnO/Al_2O_3 catalysts. The most common industrial feed gas composition for syngas conversion to methanol is given in Eq. (11) [28].

$$\frac{n_{H_2} - n_{CO_2}}{n_{CO} - n_{CO_2}} = 2 \tag{11}$$

Similar to the state-of-the-art methanol production from syngas, methane synthesis is mainly based on CO hydrogenation [15]. It is well known that CO_2 is detrimental to the hydrogenation to methane [30]. In feed streams with both carbon oxides, CO inhibits CO_2 hydrogenation by faster and stronger adsorption to the active Ni sites [31, 32]. To achieve comparable product yields and carbon-based

conversions to the state-of-the-art methane and methanol production from CO and syngas, the choice of suitable catalysts is crucial when the process gas from direct siderite ore reduction shall be used. As highly active industrial catalysts for CO and syngas conversion to methane and methanol are not as efficient for CO_2-rich feed streams [30, 33], the development of hydrogenation catalysts, that are capable of handling high CO_2 concentrations while being selective for methane or methanol is crucial. Moreover, for catalytic valorization of industrial off-gas in general and the process gas of the direct reduction of siderite ore in specific, catalysts need to be easy to synthesize, robust under reaction conditions, and easy to recycle.

Since high CO_2 concentrations in the feed stream are detrimental when conventional catalysts are used, the catalysts developed here were primarily tested for CO_2 hydrogenation. The decision was made on the assumption that the catalysts, when being efficient for CO_2 hydrogenation, can be applied for both CO_2-rich and CO-rich process streams. MgO carrier material was found to be an appreciable CO_2 adsorber, initiating CO_2 hydrogenation to methane by forming magnesium carbonate on the surface [24]. As MgO is a slag-former, it can easily be recycled in the blast-oxygen furnaces in the copper and steel industry and, thus, fulfills the criterion of recyclability. To prove this concept, bifunctional Ni- and Cu-based catalyst on MgO carrier material were prepared by wet impregnation and successfully applied for CO_2 hydrogenation to methane and methanol [21–23].

3.1 Materials and Methods – CO_2 Hydrogenation

For the catalytic hydrogenation experiments, hydrogen (99.999 %), CO_2 (99.998 %), and nitrogen (99.999 %) supplied by Air Liquide were used. The bifunctional Ni- and Cu-based catalysts on MgO carrier material were prepared by wet impregnation with nickel nitrate hexahydrate ($Ni(NO_3)_2{\cdot}6H_2O$, 99 %, p.a., Lactan), copper(II) nitrate trihydrate ($Cu(NO_3)_2{\cdot}3H_2O$, ≥ 99.5 %, p.a., ACS), spherical granulated MagGran© ($4MgCO_3{\cdot}Mg(OH)_2{\cdot}4H_2O$, Ph. Eur., Magnesia AG, Switzerland) with a particle size distribution of 0–8 wt %: < 150 µm, 0–15 wt %: 150–250 µm, 55–80 wt %: 250–600 µm, and deionized water. Both catalysts were prepared in four steps:

(1) Preparation of MgO: Calcination of MagGran© granulate in a muffle furnace (Heraeus M110) for 5 h in air at 723 K followed by 2 h at 823 K (Eq. (12)).

$$4MgCO_3 \cdot Mg(OH)_2 \cdot 4H_2O \rightleftharpoons 5MgO + 4CO_2 + 5H_2O \quad (12)$$

(2) Wet impregnation: The calcined MgO was impregnated with nickel or copper(II) nitrate solution, stirred in a water cooled flask for 2 h, filtered off, and dried overnight. The impregnation is described in detail in Loder et al. [22] and Kleiber et al. [23].

(3) Thermal decomposition: The Ni-based catalyst precursor was calcined in the muffle furnace for 2 h at 393 K followed by 5 h at 673 K (Eq. (13)). The Cu-based catalyst precursor was calcined for 1 h at 423 K followed by 5 h at 723 K (Eq. (14)).

$$Ni(NO_3)_2 \cdot 6H_2O \rightleftharpoons NiO + 2NO_2 + 6H_2O \quad (13)$$

$$Cu(NO_3)_2 \cdot 3H_2O \rightleftharpoons CuO + 2NO_2 + 3H_2O \quad (14)$$

(4) Reduction (catalyst activation): The NiO/MgO powder was reduced (Eq. (15)) in a tubular reactor for 4 h at 773 K with a feed gas ratio of H_2/N_2 = 90:10 (v/v) and a flow rate of 0.030 m^3h^{-1} (STP). The CuO/MgO powder was reduced (Eq. (16)) in a semi-continuous tank reactor for 3.5 h at the reaction conditions of the CO_2 hydrogenation experiments to methanol (573 K and 5 MPa). At these temperatures, reduction of NiO to elemental Ni and CuO to elemental Cu is complete.

$$NiO + H_2 \rightleftharpoons Ni + H_2O \quad \Delta_R G^0_{773K} = -45.6 \text{ kJ mol}^{-1} \quad (15)$$

$$CuO + H_2 \rightleftharpoons Cu + H_2O \quad \Delta_R G^0_{573K} = -120.3 \text{ kJ mol}^{-1} \quad (16)$$

The experiments for CO_2 hydrogenation to methane were conducted in the lab-scale fixed-bed tubular reactor from Parr Instrument Company that was used for the reduction of siderite ore. The Ni/MgO catalyst was placed in the middle of the tubular reactor. The Ni load on the Ni/MgO catalyst was varied between 11 and 27 wt %. The reaction temperature was altered between 533 at 648 K. The feed gas flow rate was investigated in a range of 0.015 to 0.060 m^3h^{-1} (STP) (space velocity of 3.75 to 15.0 $m^3h^{-1}kg^{-1}$). The feed gas ratio of H_2/CO_2 (v/v) was varied between 3:1 and 5:1. As for the direct reduction experiments, the gaseous products were monitored by an online gas analyzer with a Caldos27 thermal conductivity analyzer and an Uras26 infrared photometer from ABB. The condensable by-products were analyzed with a Shimadzu TOC-L CPH total organic carbon analyzer.

The experiments for CO_2 hydrogenation to methanol were performed in a semi-continuous tank reactor (Büchi Glas Uster Limbo350) with external condensation of condensable products and external recycle for unconverted gaseous reactants. The reactor set up is described in detail in Kleiber et al. [23]. The Cu/MgO catalyst was placed inside the reactor. The reactor was pressurized with a stoichiometric feed gas ratio (H_2/CO_2 = 3:1 (v/v)) to 5 MPa and heated to 573 K. During the 48-h lasting experiments, a constant gas flow rate of 0.01 m^3h^{-1} (STP) was induced by a gas circulation pump. The experiments were carried out in 3-h cycles, which were characterized by a decrease of the reaction pressure due to the consumption of reactants and the condensation of condensable products, followed by re-pressurizing with a stoichiometric feed of hydrogen and

CO_2 (H_2/CO_2 of 3:1) to a reaction pressure of 5 MPa. Gas samples were taken after each interval and analyzed by micro gas chromatography with an Agilent/Inficon microGC 3000. The liquid product was analyzed by a Shimadzu GC2010plus gas chromatograph with a flame ionization detector and a ZB WAXplus column with an inner diameter of 320 µm, a length of 60 m, and a thickness of 0.5 µm.

3.2 Results – Methane Synthesis

To investigate methane synthesis through CO_2 hydrogenation on Ni/MgO catalysts, the effects of Ni load (11–27 wt %), space velocity (3.75 to 15.0 $m^3h^{-1}kg^{-1}$), feed gas ratio (H_2/CO_2 from 3:1 to 5:1), and reaction temperature (533 to 648 K) were investigated at ambient pressure [21, 22]. The results are depicted in Tab. 1 and Figs. 7 and 8. The highest CO_2 conversion of 87 % with a selectivity for methane of ≥ 99 % was achieved with the 27 wt % Ni/MgO catalyst at a space velocity of 3.75 $m^3h^{-1}kg^{-1}$. The feed gas ratio of H_2/CO_2 of 5:1 resulted in the highest CO_2 conversion of ≥ 99 % at a space velocity of 3.75 $m^3h^{-1}kg^{-1}$.

At constant reaction temperature, experiments with a stoichiometric feed gas ratio (H_2/CO_2 = 4:1) and a constant space velocity of 3.75 $m^3h^{-1}kg^{-1}$ showed increasing CO_2 conversions for catalysts with increasing Ni load. At constant Ni load, the CO_2 conversion increased with increasing reaction temperature approaching the thermodynamic equilibrium conversion. The experimental parameters are listed in Tab. 1.

With increasing feed gas flow rate, the conversion of CO_2 decreased as the residence time of the reactants was shorter (Fig. 7 for 27 wt % Ni/MgO catalyst). With increasing temperature, the conversion of CO_2 increased up to 598 K and then decreased. The highest CO_2 conversion of 87 % was obtained at 598 K with a feed gas flow rate of 0.015 m^3h^{-1} (STP). The selectivity to methane (S_{CH_4}) was ≥ 99 % in all experiments.

The effect of the feed gas ratio on the conversion of CO_2 was investigated for feed gas ratios of H_2/CO_2 of 3:1 to 5:1 and various feed gas flow rates (Fig. 8 for 27 wt % Ni/MgO catalyst at 598 K). The CO_2 conversion increased with decreasing feed gas flow rate for all feed gas ratios.

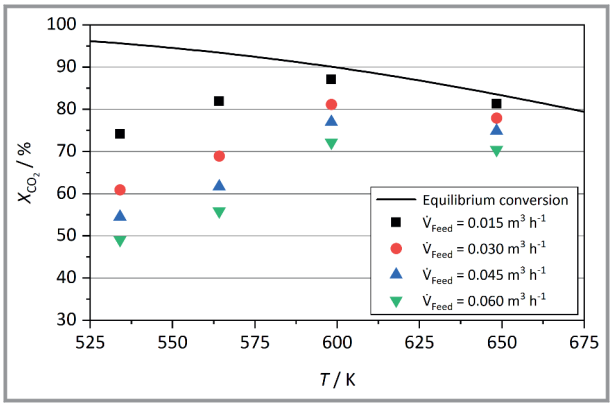

Figure 7. Effect of the reaction temperature and the feed gas flow rate on CO_2 conversion for CO_2 hydrogenation to methane with a bifunctional Ni/MgO catalyst (27 wt % Ni). Process conditions: feed gas ratio of H_2/CO_2 = 4:1 (v/v), catalyst mass m_{Cat} = 4.0 g, space velocity of 3.75 to 15.0 $m^3h^{-1}kg^{-1}$. The temperature is shown as mean values with a standard deviation of ±0.8 %. The CO_2 conversions are also shown as mean values with a standard deviation of ±1.5 %.

With the experimental results, a kinetic reaction model based on a Langmuir-Hinshelwood rate law was developed by Loder et al. [22] (Eq. (17)). In the kinetic model, the bifunctional catalytic action of the Ni/MgO catalysts was considered. For all Ni/MgO catalysts, the activation energy

Table 1. Experimental parameters for catalytic CO_2 hydrogenation to methane with Ni/MgO catalysts; ambient pressure, stoichiometric feed gas ratio H_2/CO_2 = 4:1 (v/v).

Catalyst		Temperature	Feed gas flow rate	Space velocity	CO_2 conversion
w_{Ni} [wt %]	m [g]	T [K]	$\dot{V}_{Feed}$ [m^3h^{-1} (STP)]	[$m^3h^{-1}kg^{-1}$]	X_{CO_2} [%]
27	4.0	533	0.015	3.75	74.2
27	4.0	563	0.015	3.75	81.9
27	4.0	598	0.015	3.75	87.1
27	4.0	648	0.015	3.75	81.3
21	4.0	533	0.015	3.75	56.8
21	4.0	563	0.015	3.75	74.2
21	4.0	598	0.015	3.75	79.9
21	4.0	648	0.015	3.75	77.5
17	12.0	533	0.045	3.75	17.9
17	12.0	563	0.045	3.75	41.4
17	12.0	598	0.045	3.75	70.0
17	12.0	648	0.045	3.75	77.7
11	12.0	533	0.045	3.75	18.8
11	12.0	563	0.045	3.75	27.5
11	12.0	598	0.045	3.75	45.5
11	12.0	648	0.045	3.75	71.9

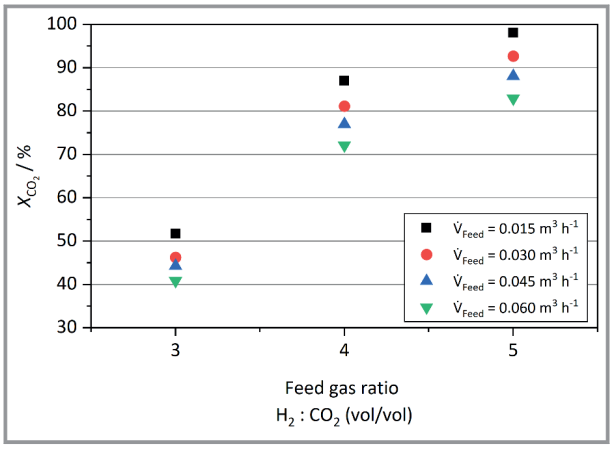

Figure 8. Effect of the volumetric feed gas ratio H_2/CO_2 on CO_2 conversion with a bifunctional Ni/MgO catalyst (27 wt % Ni). Process conditions: reaction temperature: T = 598 K, ambient pressure, catalyst mass m_{Cat} = 4.0 g, space velocity of 3.75 to 15.0 $m^3h^{-1}kg^{-1}$. The temperature is shown as mean values with a standard deviation of ±0.8 %. The CO_2 conversions are also shown as mean values with a standard deviation of ±1.5 %.

was constant and the frequency factor correlated linearly with the Ni load [22]. This led to the assumptions that different Ni load does not have an effect on the reaction mechanism, but the activity of the Ni/MgO catalysts depends on the number of available Ni sites. For the by-product water, a retarding effect on the rate of reaction was found.

$$\frac{dX_{CO_2}}{dt} = \frac{k_{for}\, c_{CO_2} c_{H_2} - k_{rev}\, c_{CH_4} c_{H_2O}}{1 + K_{H_2O}\, c_{H_2O}} \quad (17)$$

The study demonstrated the high efficiency and selectivity of the Ni/MgO catalysts for methane synthesis from CO_2. A further study from Baldauf-Sommerbauer et al. [21] showed good results regarding the long-term stability of the catalysts, which render them promising catalysts for CO_2 valorization to methane. Methane synthesis in the process gas from direct reduction of siderite ore does not only prevent CO_2 emissions during iron production but also provides an efficient means for hydrogen storage as methane may act as hydrogen-based energy carrier [34]. Additionally, the main advantage of Ni catalysts with MgO carrier material, direct recycling of spent catalyst in the oxygen blast furnace, has to be outlined.

3.3 Results – Methanol Synthesis

For methanol synthesis by CO_2 hydrogenation, the activity of Cu/MgO catalysts (38 wt % Cu) was investigated in 48-h experiments that were split in 3-h cycles (intervals) at 573 K and 5 MPa. Within the first 24 h of the experiments, increasing amount of CO was formed up to a volumetric fraction of 16 vol %. In the following 24 h of the experiments, the volumetric fractions of hydrogen, CO, and CO_2 did not change significantly. Based on the gas phase compositions, the hydrogen and CO_2 conversions and CO and methanol selectivities were calculated for each interval and the overall experiment. An overall relative CO_2 conversion (X_{CO_2}) of 76 % and an overall methanol selectivity (S_{CH_3OH}) of 59 % were obtained with the 38 wt % Cu/MgO catalyst. The results showed that steady-state operation was not fully achieved during the experiment, as the interval selectivity for methanol steadily increased up to 88 % in the last interval (Fig. 9). The Cu/MgO catalyst showed high potential

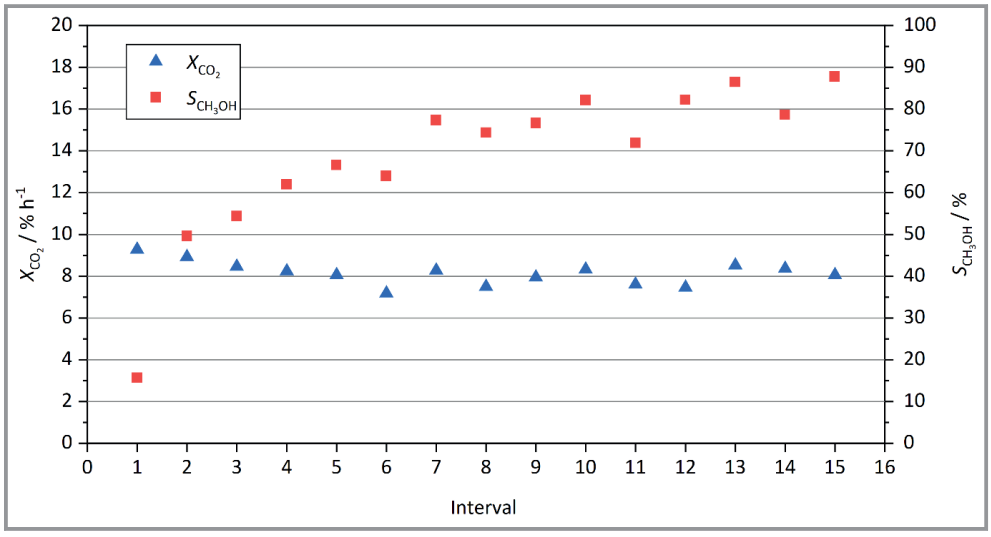

Figure 9. CO_2 conversion normalized by the interval time and methanol selectivity for methanol synthesis by CO_2 hydrogenation with a bifunctional 38 wt % Cu/MgO catalyst in a semi-continuous tank reactor with external condensation and recycle of unconverted gaseous reactants. Process conditions: reaction time t = 48 h, reaction temperature T = 573 K, reaction pressure P = 5 MPa, feed gas ratio of H_2/CO_2 = 3:1 (v/v). The normalized CO_2 conversion and methanol selectivity are shown as mean values with a standard deviation of ±1.5 %.

and high catalytic activity for CO_2 hydrogenation and even increased its selectivity during operation. This enables Cu/MgO catalysts to be used for the catalytic hydrogenation of the CO/CO_2-rich process gas from direct reduction of siderite ore. Spent Cu/MgO catalysts are easily recycled in the copper blast furnace.

Methanol synthesis by catalytic hydrogenation of the CO/CO_2-rich process gas from direct reduction of siderite ore substantially decreases CO_2 emissions in the novel iron production pathway. This process step may contribute decisively to fossil-free methanol production and improves the energy density as a hydrogen-based energy carrier by one order of magnitude [35].

4 Summary and Conclusion

A holistic technology concept for CO_2 emission mitigation in iron production from siderite ore was proposed. When the conventional two-step iron production route with calcination of siderite ore to hematite and consecutive reduction in the blast furnace is circumvented by a one-step direct reduction process with hydrogen, CO_2 emissions drop by more than 60 %. Compared to hematite reduction with hydrogen, the amount of the reducing agent hydrogen is reduced by 33 % when siderite is directly reduced. Valorization of the process gas, mainly consisting of unconverted hydrogen, CO, and CO_2, by catalytic hydrogenation to methane and methanol enables the production of iron from siderite ore to proceed with low CO_2 emissions. With green hydrogen, it gives access to fossil-free production of methane and methanol, and thus, hydrogen-based energy carriers with improved energy densities.

During direct reduction of siderite ore, complete conversion of the iron-bearing components siderite and ankerite was possible with a degree of metallization of > 80 % at a reduction temperature of 873 K. At elevated reaction temperature of 1023 K, the degree of metallization increased to 92 %. Neither variation of the feed gas ratio of H_2/N_2 from 90:10 to 55:45 (v/v) nor the admixture of methane (15–80 vol %) showed a significant effect on the degree of metallization. The admixture of CO_2 (27–63 vol %) to the feed gas stream favored magnetite formation instead and, thereby, decreased the degree of metallization. Precise adaption of the process parameters reduction temperature and feed gas composition allow for assembling a tailor-made process gas with specific CO_2/CO ratios.

For further valorization of the process gas, catalytic CO_2 hydrogenation to methane and methanol was suggested with bifunctional Ni/MgO and Cu/MgO catalysts, respectively. These bifunctional catalysts showed high catalytic activity and selectivity for methane and methanol in CO_2 conversion. In the next step, the catalytic activity of both bifunctional catalysts will be validated for CO-containing process gas from direct siderite ore reduction.

The combination of the novel direct reduction process with catalytic hydrogenation of mixed CO/CO_2 process gas streams to methane and methanol using catalysts on MgO carrier material provides a complete technology concept for CO_2 emission-lean iron production from siderite ore. It enables resources to be used efficiently and allows to close the material cycle through valorization of the process gas and recyclability of spent catalyst material.

Supporting Information

Supporting Information for this article can be found under DOI: https://doi.org/10.1002/cite.202100189.

The project "DiREkt – Direct reduction of iron carbonate" was funded by the Austrian "Klima- und Energiefonds" in the framework of the program "Energieforschungsprogramm 4. Ausschreibung". The authors wish to thank A. Stadtschnitzer and A. Kogelbauer from VA Erzberg GmbH for their valuable collaboration and support in the project. The authors gratefully acknowledge the support from the NAWI Graz program. Thanks are also due to C. Winter for his support with laboratory work.

Symbols used

c	[mol L^{-1}]	molar concentration
$\Delta_R G_T^0$	[kJ mol^{-1}]	standard Gibbs free energy of reaction at temperature T
$\Delta_R H^0$	[kJ mol^{-1}]	enthalpy of reaction
K	[–]	equilibrium constant
m	[g]	mass
n	[mol]	amount of substance
P	[MPa]	pressure
S	[%]	selectivity
t	[h]	(reaction) time
T	[K]	temperature
$\dot{V}$	[$m^3 h^{-1}$]	volumetric gas stream
$w_{Fe,met}$	[wt %]	degree of metallization
X	[%]	relative conversion

Greek letter

φ	[vol %]	volumetric gas composition

Sub- and superscripts

a, b, c, d, 1–x	stoichiometric coefficients
cat	catalyst
Fe,met	elemental (metallic) iron

Fe,tot	total iron
for	forward
rev	reverse
sid	siderite

Abbreviation

RWGS	reverse water-gas shift

References

[1] *Climate Change 2014: Impacts, Adaptation, and Vulnerability. Part A: Global and Sectoral Aspects. Contribution of Working Group II to the Fifth Assessment Report of the Intergovernmental Panel on Climate Change* (Eds: C. B. Field, V. R. Barros, D. J. Dokken, K. J. Mach, M. D. Mastrandrea, T. E. Bilir, M. Chatterjee, K. L. Ebi, Y. O. Estrada, R. C. Genova, B. Girma, E. S. Kissel, A. N. Levy, S. MacCracken, P. R. Mastrandrea, L. L. White), Cambridge University Press, Cambridge **2014**.

[2] *Climate Change 2021: The Physical Science Basis. Contribution of Working Group I to the Sixth Assessment Report of the Intergovernmental Panel on Climate Change* (Eds: V. Masson-Delmotte, P. Zhai, A. Pirani, S. L. Connors, C. Péan, S. Berger, N. Caud, Y. Chen, L. Goldfarb, M. I. Gomis, M. Huang, K. Leitzell, E. Lonnoy, J. B. R. Matthews, T. K. Maycock, T. Waterfield, O. Yelekçi, R. Yu, B. Zhou), Cambridge University Press, Cambridge, in press.

[3] *Steel Statistical Yearbook 2021*, World Steel Association, Brussels **2021**.

[4] T. Ariyama, K. Takahashi, Y. Kawashiri, T. Nouchi, Diversification of the Ironmaking Process Toward the Long-Term Global Goal for Carbon Dioxide Mitigation, *J. Sustainable Metall.* **2019**, *5*, 276–294. DOI: https://doi.org/10.1007/s40831-019-00219-9

[5] M. Wörtler, F. Schuler, N. Voigt, T. Schmidt, P. Dahlmann, H. B. Lüngen, J. Ghenda, *Steel's Contribution to a Low-Carbon Europe 2050*, The Boston Consulting Group, Boston, MA **2013**.

[6] G. Baldauf-Sommerbauer, S. Lux, M. Siebenhofer, Sustainable Iron Production from Mineral Iron Carbonate and Hydrogen, *Green Chem.* **2016**, *18*, 6255–6265. DOI: https://doi.org/10.1039/C6GC02160C

[7] S. Lux, G. Baldauf-Sommerbauer, B. Ottitsch, A. Loder, M. Siebenhofer, Iron Carbonate Beneficiation through Reductive Calcination – Parameter Optimization to Maximize Methane Formation, *Eur. J. Inorg. Chem.* **2019**, *2019*, 1748–1758. DOI: https://doi.org/10.1002/ejic.201801394

[8] S. Lux, G. Baldauf-Sommerbauer, M. Siebenhofer, Hydrogenation of Inorganic Metal Carbonates: A Review on Its Potential for Carbon Dioxide Utilization and Emission Reduction, *ChemSusChem* **2018**, *11*, 3357–3375. DOI: https://doi.org/10.1002/cssc.201801356

[9] G. Baldauf-Sommerbauer, S. Lux, W. Aniser, M. Siebenhofer, Synthesis of Carbon Monoxide from Hydrogen and Magnesite/Dolomite, *Chem. Ing. Tech.* **2017**, *89*, 172–179. DOI: https://doi.org/10.1002/cite.201600078

[10] J. Schneidewind, M. A. Argüello Cordero, H. Junge, S. Lochbrunner, M. Beller, Two-Photon, Visible Light Water Splitting at a Molecular Ruthenium Complex, *Energy Environ. Sci.* **2021**, *14*, 4427–4436. DOI: https://doi.org/10.1039/D1EE01053K

[11] M. Svanberg, J. Ellis, J. Lundgren, I. Landälv, Renewable Methanol as a Fuel for the Shipping Industry, *Renewable Sustainable Energy Rev.* **2018**, *94*, 1217–1228. DOI: https://doi.org/10.1016/j.rser.2018.06.058

[12] S. Verhelst, J. W. G. Turner, L. Sileghem, J. Vancoillie, Methanol as a Fuel for Internal Combustion Engines, *Prog. Energy Combust. Sci.* **2019**, *70*, 43–88. DOI: https://doi.org/10.1016/j.pecs.2018.10.001

[13] V. Tola, F. Lonis, Low CO_2 Emissions Chemically Recuperated Gas Turbines Fed by Renewable Methanol, *Appl. Energy* **2021**, *298*, 117146. DOI: https://doi.org/10.1016/j.apenergy.2021.117146

[14] W. H. Day, Methanol Fuel in Commercial Operation on Land and Sea, *Gas Turbine World* **2016**, *November–December 2016*, 16–21.

[15] I. Kuznecova, J. Gusca, Property Based Ranking of CO and CO_2 Methanation Catalysts, *Energy Procedia* **2017**, *128*, 255–260. DOI: https://doi.org/10.1016/j.egypro.2017.09.068

[16] T. an Le, M. S. Kim, S. H. Lee, T. W. Kim, E. D. Park, CO and CO_2 Methanation over Supported Ni Catalysts, *Catal. Today* **2017**, *293–294*, 89–96. DOI: https://doi.org/10.1016/j.cattod.2016.12.036

[17] N. D. Nielsen, J. Thrane, A. D. Jensen, J. M. Christensen, Bifunctional Synergy in CO Hydrogenation to Methanol with Supported Cu, *Catal. Lett.* **2020**, *150*, 1427–1433. DOI: https://doi.org/10.1007/s10562-019-03036-7

[18] S. Zander, E. L. Kunkes, M. E. Schuster, J. Schumann, G. Weinberg, D. Teschner, N. Jacobsen, R. Schlögl, M. Behrens, The Role of the Oxide Component in the Development of Copper Composite Catalysts for Methanol Synthesis, *Angew. Chem., Int. Ed.* **2013**, *52*, 6536–6540. DOI: https://doi.org/10.1002/anie.201301419

[19] V. D. Dasireddy, B. Likozar, The Role of Copper Oxidation State in $Cu/ZnO/Al_2O_3$ Catalysts in CO_2 Hydrogenation and Methanol Productivity, *Renewable Energy* **2019**, *140*, 452–460. DOI: https://doi.org/10.1016/j.renene.2019.03.073

[20] V. D. Dasireddy, N. S. Štefančič, M. Huš, B. Likozar, Effect of Alkaline Earth Metal Oxide (MO) $Cu/MO/Al_2O_3$ Catalysts on Methanol Synthesis Activity and Selectivity via CO_2 Reduction, *Fuel* **2018**, *233*, 103–112. DOI: https://doi.org/10.1016/j.fuel.2018.06.046

[21] G. Baldauf-Sommerbauer, S. Lux, W. Aniser, B. Bitschnau, I. Letofsky-Papst, M. Siebenhofer, Steady-State and Controlled Heating Rate Methanation of CO_2 on Ni/MgO in a Bench-Scale Fixed Bed Tubular Reactor, *J. CO_2 Util.* **2018**, *23*, 1–9. DOI: https://doi.org/10.1016/j.jcou.2017.10.022

[22] A. Loder, M. Siebenhofer, S. Lux, The Reaction Kinetics of CO_2 Methanation on a Bifunctional Ni/MgO Catalyst, *J. Ind. Eng. Chem.* **2020**, *85*, 196–207. DOI: https://doi.org/10.1016/j.jiec.2020.02.001

[23] S. Kleiber, M. Pallua, M. Siebenhofer, S. Lux, Catalytic Hydrogenation of CO_2 to Methanol over Cu/MgO Catalysts in a Semi-Continuous Reactor, *Energies* **2021**, *14*, 4319. DOI: https://doi.org/10.3390/en14144319

[24] H. Y. Kim, H. M. Lee, J.-N. Park, Bifunctional Mechanism of CO_2 Methanation on $Pd\text{-}MgO/SiO_2$ Catalyst: Independent Roles of MgO and Pd on CO_2 Methanation, *J. Phys. Chem. C* **2010**, *114*, 7128–7131. DOI: https://doi.org/10.1021/jp100938v

[25] H. Li, H. Tian, S. Chen, Z. Sun, T. Liu, R. Liu, S. Assabumrungrat, J. Saupsor, R. Mu, C. Pei, J. Gong, Sorption Enhanced Steam Reforming of Methanol for High-Purity Hydrogen Production over $Cu\text{-}MgO/Al_2O_3$ Bifunctional Catalysts, *Appl. Catal., B* **2020**, *276*, 119052. DOI: https://doi.org/10.1016/j.apcatb.2020.119052

[26] A. Loder, M. Siebenhofer, A. Böhm, S. Lux, Clean Iron Production through Direct Reduction of Mineral Iron Carbonate with Low-Grade Hydrogen Sources; the Effect of Reduction Feed Gas Composition on Product and Exit Gas Composition, *Cleaner Eng. Technol.* **2021**, *5*, 100345. DOI: https://doi.org/10.1016/j.clet.2021.100345

[27] S. Rönsch, J. Köchermann, J. Schneider, S. Matthischke, Global Reaction Kinetics of CO and CO_2 Methanation for Dynamic Process Modeling, *Chem. Eng. Technol.* **2016**, *39*, 208–218. DOI: https://doi.org/10.1002/ceat.201500327
[28] M. Bertau, H. Offermanns, L. Plass, F. Schmidt, H.-J. Wernicke, *Methanol: The Basic Chemical and Energy Feedstock of the Future*, Springer, Berlin **2014**.
[29] *HSC Chemistry® Software*, Outotec Technologies, Tampere **2018**.
[30] B. Miao, S. S. K. Ma, X. Wang, H. Su, S. H. Chan, Catalysis Mechanisms of CO_2 and CO Methanation, *Catal. Sci. Technol.* **2016**, *6*, 4048–4058. DOI: https://doi.org/10.1039/C6CY00478D
[31] T. Burger, P. Donaubauer, O. Hinrichsen, On the Kinetics of the Co-Methanation of CO and CO_2 on a Co-Precipitated Ni-Al Catalyst, *Appl. Catal., B* **2021**, *282*, 119408. DOI: https://doi.org/10.1016/j.apcatb.2020.119408
[32] T. van Herwijnen, H. van Doesburg, W. A. de Jong, Kinetics of the Methanation of CO and CO_2 on a Nickel Catalyst, *J. Catal.* **1973**, *28*, 391–402. DOI: https://doi.org/10.1016/0021-9517(73)90132-2
[33] R. Raudaskoski, E. Turpeinen, R. Lenkkeri, E. Pongrácz, R. L. Keiski, Catalytic Activation of CO_2: Use of Secondary CO_2 for the Production of Synthesis Gas and for Methanol Synthesis over Copper-Based Zirconia-Containing Catalysts, *Catal. Today* **2009**, *144*, 318–323. DOI: https://doi.org/10.1016/j.cattod.2008.11.026
[34] U. Bossel, Does a Hydrogen Economy Make Sense?, *Proc. IEEE* **2006**, *94*, 1826–1837. DOI: https://doi.org/10.1109/JPROC.2006.883715
[35] B. Gurau, E. S. Smotkin, Methanol Crossover in Direct Methanol Fuel Cells: A Link between Power and Energy Density, *J. Power Sources* **2002**, *112*, 339–352. DOI: https://doi.org/10.1016/S0378-7753(02)00445-7

